HNUE JOURNAL OF SCIENCE DOI: 10.18173/2354-1059.2019-0080
Natural Sciences 2019, Volume 64, Issue 10, pp. 114-122
This paper is available online at http://stdb.hnue.edu.vn

PREPARATION AND CHARACTERIZATION OF ZINC HIDROXYAPATITE COATINGS ON 316L STAINLESS STEEL

Vo Thi Hanh[1,2], Ha Manh Hung[1], Le Thi Duyen[1,2] and Dinh Thi Mai Thanh[3]
[1]*Faculty of Chemistry, Hanoi University of Mining and Geology*
[2]*Centre for Excellence in Annalysis and Experiment, Hanoi University of Mining and Geology*
[3]*University of Science and Technology of Hanoi, Vietnam Academy of Science and Technology*

Abstract. Zinc hydroxyapatite coatings (ZnHAp) were synthesized on 316L stainless steel by ion exchange method between hydroxyapatite coatings (HAp) and solution containing $Zn(NO_3)_2$. Effect of the initial concentration of Zn^{2+} and contact time to ion exchange process was studied. The analytical results of FTIR, SEM, Xray, and AAS showed that the obtained coatings were single phase crystals of HAp, and the present of Zn in HAp structure with the atomic ratios of Zn/Ca, (Ca + Zn)/P of 0.143 and 1.707 changed the morphology, the crystal diameter and the lattice parameters. Besides, kinetics of ion exchange process followed the model of the pseudo-second order kinetic with the ion exchange capacity at equilibrium of 1.529 mmol/g and the rate constant of 0.112 g/mmol.min.

Keywords: 316L stainless steel; hydroxyapatite coatings (HAp); zinc hydroxyapatite coatings (ZnHAp); ion exchange.

1. Introduction

Hydroxyapatite (HAp) is the main component in natural bones, accounts for 25-75% by weight and 35-65% by volume [1]. Synthetic HAp has a Ca/P ratio of 1.67, similar to that in natural bones and it has excellent biological activity hence it is extensively studied and applied in the biomedical field [2, 3]. HAp coatings are covered on metal and alloy surfaces such as Ti, 316L stainless steel (316LSS) to improve the quality and biocompatibility [4, 5]. When implanted, the HAp coatings are capable of creating a tight bond between the host's bone and the implant material, accelerating bone healing.

However, the biggest concern was postoperative infection after implantation. Therefore, scientists were very interested in bringing the antimicrobial agents to the implant. In addition, inorganic antimicrobial agents, including copper, silver and zinc

Received September 25, 2019. Revised October 22, 2019. Accepted October 29, 2019.
Contact Vo Thi Hanh, e-mail address: vothihanh@humg.edu.vn

ions, are well-respected by scientists for their stability and safety [1]. They not only reduce the adhesion of bacteria to the surface of the implants, but also have the ability to inhibit their growth [6].

Zinc is a necessary trace element in the body. The presence of Zn in the bone stimulates bone formation and inhibits the process of bone destruction. Moreover, zinc is known for its broad spectrum antibacterial activity against Gram-positive and Gram-negative bacteria, fungi, protozoa, viruses, and even antibiotic-resistant strains [6, 7]. ZnHAp coatings with 1.6% Zn in mass deposited on 304 stainless steel have shown increased biological activity, antibacterial activity, and non-toxicity to cells [7]. The researcher Y.L. Jeyachandran (Indian) has investigated the development of P. gingivalis in FHAp, ZnFHAp and TiN coatings. The results exhibited that the bacterial inhibition of ZnFHAp coatings is greater than that of FHAp coatings and exceeded that of TiN coatings [8].

In this paper, we introduce synthesis results of ZnHAp coatings on 316L stainless steel by ion exchange method between HAp coatings and solutions containing Zn^{2+} ions. The characterization of the obtained ZnHAp coatings was studied by IR, Xray, SEM, AAS.

2. Content

2.1. Experiments

2.1.1. Electrodepositon HAp coating on 316L stainless steel

316L Stainless steel (316LSS) with the chemical composition: 0.27% Al; 0.17% Mn, 0.56% Si, 17.98% Cr, 9.34% Ni, 2.15% Mo, 0.045% P, 0.035% S and 69.45% Fe was used as the substrate and a cathode (working electrode) for the experiments. It is sized of 1x10x0.2 cm and limited work area of 1cm2 by epoxy. Afterwards, the sample was coated with the HAp coatings by cathodic scanning potential method at scanning potential ranges 0 ÷ -1.7 V/SCE; scanning rates 5 mV/s; temperature 50oC; the process was repeated 5 times in a solution contained $3x10^{-2}$ M $Ca(NO_3)_2$ + $1.8x10^{-2}$ M $NH_4H_2PO_4$ + $6x10^{-2}$ M $NaNO_3$.

The electrodeposition was carried out in a three-electrode cell with 316LSS as the working electrode; platinum foil electrode acting as the counter electrode and a saturated calomel electrode (SCE) as the reference electrode by the Autolab PGSTAT 30 equipment (Holland).

2.1.2. Synthesis of ZnHAp coatings

In order to choose the optimal initial concentration of Zn^{2+} and the suitable contact time for sysnthesis ZnHAp coating, material of HAp coated on 316LSS (HAp/316LSS) substrate with mass of 2,45 mg was immersed in 4mL of solution $Zn(NO_3)_2$ with variable concentrations: 0.01, 0.05, 0.10, 0.15 and 0.20 M and at differents times: 0, 2.5, 5, 10, 20, 30, 60 and 80 minutes at room temperature. Next, the material was taken out of the solution, then rinsed with sterile water and left to dry in the air. The obtained solution after immerstion was investigated to determine the remaining concentration of

ion Zn^{2+} by Atomic absorption spectroscopy (AAS) method, then calculate the ion-exchange capacity according to this formula:

$$Q = \frac{C_0 - C}{m}.V.1000 \quad (1)$$

Where, Q is the ion exchange capacity (mmol/g), C_o is the initial concentration of Zn^{2+} (mol/L), C is the remaining Zn^{2+} concentration after immersion (mol/L), V is the volume of solution (L), m is mass of HAp coatings (g).

The kinetics of Zn^{2+} ion exchange process is defined by two kinetic models: pseudo-first order (Equation 2) and pseudo-second order (Equation 3) [9] . Where, Q_e and Q_t are the ion exchange capacities respectively at equilibrium and at any time t (mmol/g), k_1, k_2 are the rate constants corresponding of the pseudo-first order (min^{-1}) and pseudo-second order (g/mmol/min).

$$\ln(Q_e - Q_t) = \ln Q_e - k_1.t \quad (2)$$

$$\frac{t}{Q_t} = \frac{1}{Q_e}.t + \frac{1}{k_2.Q_e^2} \quad (3)$$

2.1.3. ZnHAp coating characterization

The functional groups of ZnHAp coatings were analyzed by Fourier Transform Infrared (FTIR) spectroscopy. The spectra were recorded in the range of 4000 - 450 cm^{-1}, with a resolution of 8 cm^{-1} by a Nicolet 6700 Spectrometer, using the KBr pellet technique. The spectra were the sum of 32 scans. The morphology of the coatings was characterized using scanning electron microscopy (SEM) using Hitachi S4800 equipment (Japan). Moreover, chemical composition of the coatings was studied and evaluated by Atomic absorption spectroscopy (AAS) method using Perkin - Elmer 3300 equipment (Ca, Zn elements) and UV-VIS method using CINTRA equipment (P element). The phase structure and crystallinity of the ZnHAp coatings were analyzed by X-ray diffraction (SIEMENS D5005 Bruker-Germany), CuKα radiation (λ = 1.54056 Å), with the following parameters: step angle of 0.03°, the scanning rate of 0.03°s^{-1}, and 2θ in a range of 10 - 70°.

The crystallite size of HAp and ZnHAp was calculated from (002) reflection in XRD pattern, using Scherrer's equation [10] (Equation 4). Where, D (nm) is crystallite size, λ is the wavelength of the X-ray radiation (CuKα), θ (rad) is the diffraction angle, and B is the full width at half-maximum FWHM (rad) of the peak along (002) direction. Beside, lattice parameters (a, b, c) were calculated from peak (002) and (211) of XRD pattern according to equation 5. Where, d is determined from XRD, which is the distance between adjacent planes in the set of Miller indices (hkl) [11].

$$D = \frac{0,9\lambda}{\mathrm{B}.\cos\theta} \quad (4)$$

$$\frac{1}{d^2} = \frac{\frac{4}{3}(h^2 + kh + k^2)}{a^2} + \frac{l^2}{c^2} \quad (5)$$

2.2. Results and discussion

2.2.1. Effects of Zn^{2+} concentration

The ion exchange capacity depending on the initial concentrations of Zn^{2+} is shown in Figure 1. With the increase of the Zn^{2+} concentration in the solution, the ion exchange capacity increase. The initial concentrations of Zn^{2+} increase from 0.01 ÷ 0.1M, the ion -exchange capacities rise rapidly from 0.499 to 1.830 mmol/g. When the concentrations of Zn^{2+} are elevated to 0.1 and 0.2M, the capacities alter slightly (3.858 and 4.195 mmol/g). This result can be explained that the ion exchange process is reached equilibrium. Therefore, the solution with initial concentration of 0.1M Zn^{2+} is used to synthesize ZnHAp coatings.

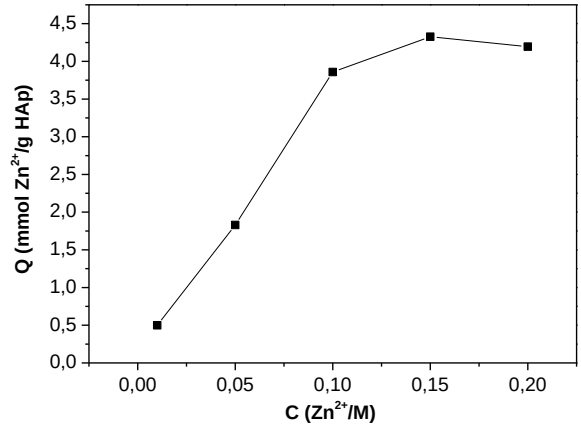

Figure 1. The change in ion exchange capacity of the HAp coatings with ion Zn^{2+} following the intinal Zn^{2+} concentration at the contact time of 30 minutes

2.2.2. Effect of the contact time

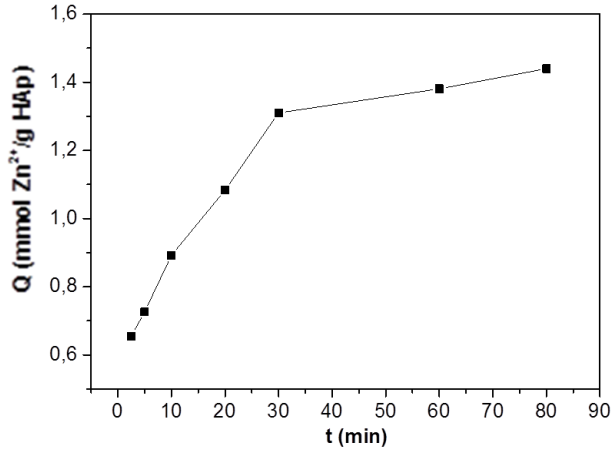

Figure 2. The change in ion exchange capacity of the HAp coatings with 0.1M Zn^{2+} solutions following the contact time at the temperature of 25^{o}C

The change of ion exchange capacity of the HAp coatings with 0.1M Zn^{2+} solutions are presented in Figure 2. During the 2.5 to 80 minutes period, the ion exchange capacity increases dramatically in the first 30 minutes (increases from 0.655 to 1.310 mmol/g), then in the period of 30 to 80 minutes the changes were not much difference (from 1.310 to 1.440 mmol/g). Therefore, the 30 minutes period is considered to be the equilibrium time and is selected for the time synthesis of ZnHAp coatings.

2.2.3. Characterization of ZnHAp coatings

The ZnHAp coatings were synthesized by immersion HAp coatings in 0.1M Zn^{2+} for 30 minutes. Then, the samples were washed, dried and determined of structure, phase, composition and mophology by IR, XRay, SEM, UV-Vis and AAS methods.

**** FTIR spectrum***

Figure 3 shows the FTIR spectra in the wavenumber range from 4000 cm^{-1} to 450 cm^{-1} of HAp and ZnHAp coatings. The results shows that the obtained ZnHAp coatings have not significant differences in FTIR spectra with HAp coatings. There are some characteristic peaks of HAp such as PO_4^{3-} and OH^-. The peaks of PO_4^{3-} group are observed at 1034, 602, 565 and 447 cm^{-1}; the vibration of OH^- are observed at 3430 and 1643 cm^{-1}. Furthermore, the peaks of NO_3^- is also detected at 1390 cm^{-1} because NO_3^- ions are presented in the electrolyte of synthetic HAp coatings. However, after immersing HAp coatings in Zn^{2+} solution for 30 minutes, NO_3^- ions are dissolved into solution so that there are no peak of NO_3^- group in the IR spectra of ZnHAp coatings.

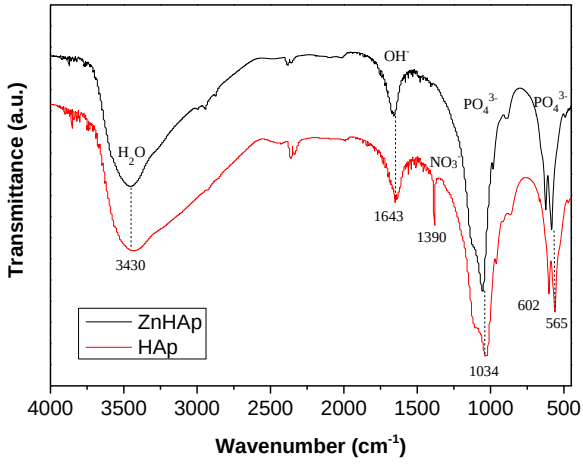

Figure 3. The IR spectra of HAp and ZnHAp coatings

**** The components of ZnHAp coatings***

The components of obtained ZnHAp coatings are analyzed by AAS (for Ca, Zn) and UV-Vis (for P) methods and are shown in Table 1. The presence of Zn in the ZnHAp coatings is 7.39 wt.% with the atomic ratios of Zn/Ca and, (Ca + Zn)/P of 0.143 and 1.707, respectively. These results are similar to ones in HAp coating and in natural

bone (1.67). Quantitative elemental analysis indicates that the zinc is incorporated into the structure of the HAp by ion exchange with Ca^{2+} to form the ZnHAp coatings.

Table 1. The component of Ca, Zn, P in HAp and ZnHAp coatings

The coatings	Weigh (%)			The atomic ratios	
	Ca	P	Zn	Zn/Ca	(Ca + Zn)/P
HAp	33.2	16.8			1.532
ZnHAp	31.8	16.5	7.39	0.143	1.707

**** The Xray patterns***

Figure 4 shows the XRD patterns of HAp and ZnHAp coatings. Both XRD patterns exhibit the hydroxyapatite phase with two characteristic peaks at 2θ of 32° (211) and 26° (002). Besides, there are some peaks of HAp with smaller intensity at 2θ of 17° (101), 33° (300), 46° (222), and 54° (004). The characteristic peaks of 316L SS substrate are observed at 2θ ≈ 45° (Fe) and ≈ 44°, 51° (CrO.FeO.NiO). These results show that ZnHAp obtained coatings have crystals structure and single phase of HAp.

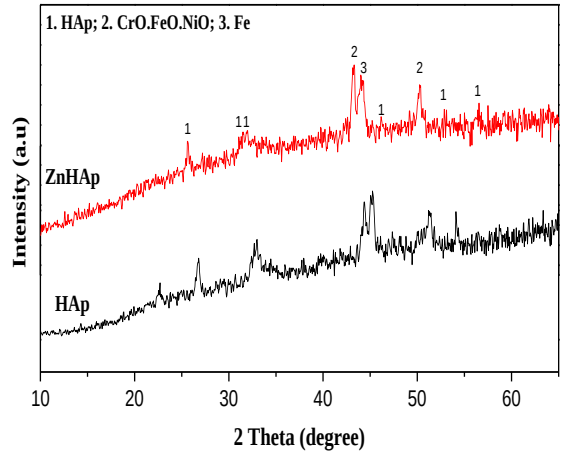

Figure 4. Xray patterns of ZnHAp and HAp coatings

The crystal diameters of HAp and ZnHAp are calculated according to Scherrer formula (Equation 4). The crystal diameter of HAp and ZnHAp coatings are about 44.2 and 22.709 nm, respectively. Table 2 presents the distance between the adjacent planes of the crystal (d) at two planes (002) and (211) and the value of the lattice parameters a, b, c of HAp and ZnHAp coatings. In comparison ZnHAp obtained coating with NIST standard of HAp sample [12] and HAp show that these values are changed: decrease corresponding for ZnHAp coatings. The results can be explained that the radius of Zn^{2+} ion (0.74 Å) is smaller than that of Ca^{2+} ion (0.99 Å); so when Zn^{2+} replace Ca^{2+} leading to reduce both the crystal diameter and the lattice parameters.

Table 2. Values of distance between the planes of the crystal and the lattice constant of ZnHAp and HAp coatings in comparision with NIST standard of HAp

	HAp [12]	HAp	ZnHAp
d(002) (Å)	3.44	3,438	3.393
d(211) (Å)	2.82	2,815	2.784
a = b (Å)	9.4451	9,426	9.325
c (Å)	6.88	6,876	6.786

**** SEM images***

SEM images of HAp and ZnHAp coating were presented in Fig. 5. The results showed that with the present of Zn in HAp structure, the morphology changes from plate shapes of HAp to coral-shapes of ZnHAp.

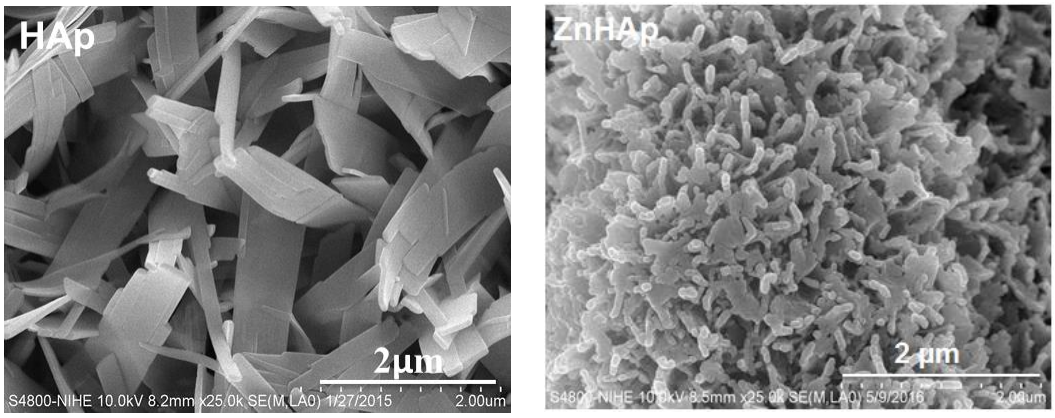

Figure 5. The SEM images of HAp and ZnHAp coatings

2.2.4. Kinetics of ion exchange

From these above results, the ratio of t/Q and $\ln(Q_e-Q_t)$ can be determined depending on the Zn^{2+} ion exchange capacity (Table 3) and the model of the pseudo-first order kinetic (Fig. 6 (1)) and pseudo-second order kinetic (Fig. 6 (2)) are established according to equation 2 and 3, respectively.

Table 3. Values of $\ln(Q_e-Q_t)$ and t/Q following the contact time

t (min)	2,5	5	10	20	30	60	80
Q_t (mmol/g)	0.655	0.726	0.892	1.083	1.310	1.381	1.440
$\ln(Q_e-Q_t)$	-0.157	-0.243	-0.481	-0.851	-1.609	-2.048	-2.659
t/Q_t (min.g/mg)	3.817	6.887	11.211	18.467	22.901	43.447	55.556

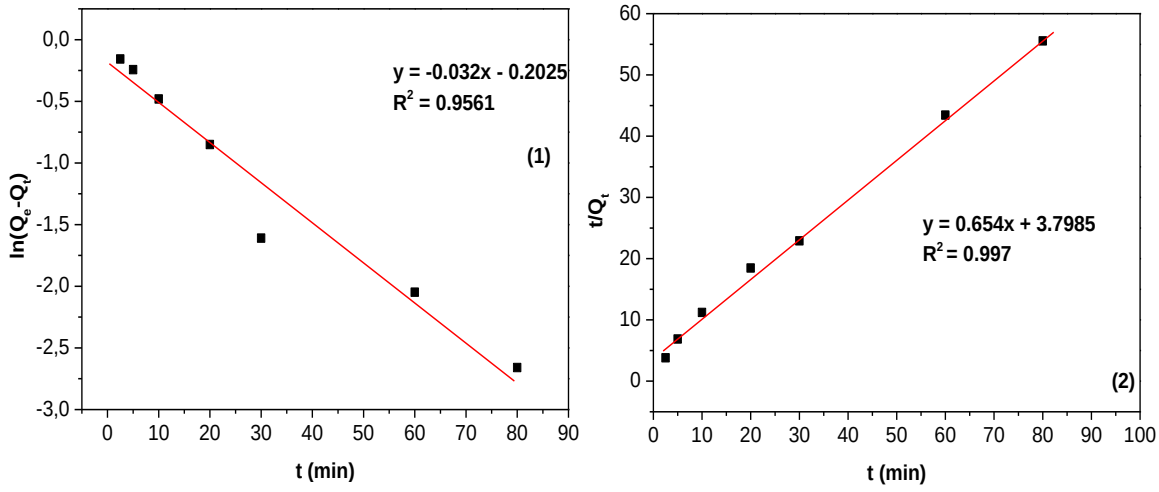

Figure 6: Model of the pseudo-first order kinetic (a) and pseudo-second order kinetic (b)

From Figure 6, the values of the adsorption rate constant (k) and the equilibrium adsorption capacity (Q_e) can be calculated. The results are presented in Table 4. Table 4 shows that the value of Q_e from pseudo-first order kinetic equation (0.817 mmol/g) differs from the experimentally obtained $Q_{e,exp}$ value (1.510 mmol/g), in this case the value of correlation coefficients R^2 = 0.956 is diverging by 1. On the contrary, the values of Q_e calculated from pseudo-second order kinetic equation (1.529 mg/g) is very little diffrent from the the experimental $Q_{e,exp}$ (1.510 mg/g), and simultaneously, the value of correlation coefficients R^2 = 0.997 is very close to 1. These results prove that the pseudo-second order kinetic equation is the best fit to the experimental data. Accordingly, the adsorption rate constant is 0.616 g/mmol/min.

Table 4. Kinetic parameters for ion exchange process between HAp coating and Zn^{2+}

Pseudo- first order			**Pseudo-second order**			$Q_{e,exp}$
Q_e (mmol/g)	k_1 (min^{-1})	R^2	Q_e (mmol/g)	k_2 (g/mmol/min)	R^2	(mmol/g)
0.817	0.032	0.8702	1.529	0.616	0.9971	1.510

3. Conclusion

ZnHAp coatings were synthesized by ion exchange method between HAp coatings with the solutions containing of Zn^{2+}. The initial concentrations 0.1M Zn^{2+} is suitable and the optimal contact time is 30 minutes for ZnHAp coatings synthesis. The obtained ZnHAp coatings have single phase crystals of HAp, coral-shapes and the content of 7.39 wt% Zn. The results of this study have widened the prospect of application of

ZnHAp coatings as a good implant material, in particular the presence of Zn in the HAp structure will increase the antibacterial and bioaccumulative properties.

REFERENCES

[1] Sumathi Shanmugam, Buvaneswari Gopal, 2014. *Copper substituted hydroxyapatite and fluorapatite: Synthesis, characterization and antimicrobial properties.* Ceramics International, 40, 10- Part A, pp. 15655-15662.

[2] Đào Quốc Hương, Phan Thị Ngọc Bích, 2007. *Tổng hợp bột hydroxyapatite kích thước nano bằng phương pháp kết tủa hoá học.* Tạp chí Hoá học, 45**,** 2, pp. 147-151.

[3] Laranjeira M.C.M. Donadel K., Goncalves V.L., F´avere V.T., 2004. *Structural, Vibrational and Mechanical Studies of Hydroxyapatite Produced by Wetchemical Methods.* Universidade Federal de Santa Catarina, Florian´opolis, Brazil, Cx.P, **476,** pp. 880-900.

[4] M. M. Dewidar, Khalil, K. A., and Lim, J. K, 2007. *Processing and mechanical properties of porous 316L stainless steel for biomedical applications.* Transactions of Nonferrous Metals Society of China, **17,** pp. 468-473.

[5] R.Q. Reis V.A. Alves, I.C.B. Santos, D.G. Souza, T. de F. Gonçalves, M.A. Pereira-da-Silva, A. Rossi, L.A. da Silva, 2009. *In situ impedance spectroscopy study of the electrochemical corrosion of Ti and Ti-6Al-4V in simulated body fluid at 25^{0}C and 37^{0}C.* Corrosion Science, **51,** pp. 2473-2482.

[6] Vojislav Stanić, Suzana Dimitrijević, Jelena Antić-Stanković, Miodrag Mitrić, Bojan Jokić, Ilija B. Plećaš, Slavica Raičević, 2010. *Synthesis, characterization and antimicrobial activity of copper and zinc-doped hydroxyapatite nanopowders.* Applied Surface Science, **256,** 20, pp. 6083-6089.

[7] Guangfei Sun, Jun Ma, and Shengmin Zhang, 2014. *Electrophoretic deposition of zinc-substituted hydroxyapatite coatings.* Materials Science and Engineering: C, **39,** pp. 67-72.

[8] Sa.K. Narayandass Y.L. Jeyachandran, D. Mangalaraj , C.Y. Bao,W.Li, Y.M. Liao, C.L. Zhang, L.Y. Xiao, W.C. Chen, 2006. *A study on bacterial attachment on titanium and hydroxyapatite based films,.* Surface & Coatings Technology, **201,** pp. 3462-3474.

[9] Y.S. Ho, G. McKay, 1999. *Pseudo-second order model for sorption processes.* Process Biochem, **34,** pp. 451-465.

[10] Pham Thi Nam Dinh Thi Mai Thanh, Nguyen Thu Phuong, Le Xuan Que, Nguyen Van Anh, Thai Hoang, Tran Dai Lam, 2013. *Controlling the electrodeposition, morphology and structure of hydroxyapatite coating on 316L stainless steel.* Materials Science and Engineering **C, 33,** 4, pp. 2037-2045.

[11] Eric KL, National Institute of Standards & Technology, Certificate of Analysis, 2008. *Standard Reference Material® 2910a, Calcium Hydroxyapatite*, (American Dental Association Foundation, U.S).